Article

Development of a Novel Anti-CD44 variant 6 Monoclonal Antibody for Multiple Applications against Colorectal Carcinomas

Ryo Ejima [1,#], Hiroyuki Suzuki [1,*,#], Tomohiro Tanaka [3], Teizo Asano [3], Mika K. Kaneko [3] and Yukinari Kato [1,3,*]

[1] Department of Molecular Pharmacology, Tohoku University Graduate School of Medicine, 2-1 Seiryo-machi, Aoba-ku, Sendai 980-8575, Miyagi, Japan; ejima.ryo.s4@dc.tohoku.ac.jp (R.E.); tomohiro.tanaka.b5@tohoku.ac.jp (T.T.)

[2] Department of Antibody Drug Development, Tohoku University Graduate School of Medicine, 2-1 Seiryo-machi, Aoba-ku, Sendai 980-8575, Miyagi, Japan; teizo.asano.a7@tohoku.ac.jp (T.A.); k.mika@med.tohoku.ac.jp (M.K.K.)

* Correspondence: hiroyuki.suzuki.b4@tohoku.ac.jp (H.S.); yukinari.kato.e6@tohoku.ac.jp (Y.K.); Tel.: +81-22-717-8207 (H.S. and Y.K.)

\# contributed equally to this work

Abstract: CD44 is a cell surface glycoprotein, and its isoforms are produced by the alternative splicing with the standard and variant exons. The CD44 variant exon containing isoforms (CD44v) are overexpressed in carcinomas. CD44v6 is one of the CD44v, and its overexpression predicts poor prognosis in colorectal cancer (CRC) patients. CD44v6 plays critical roles in CRC adhesion, proliferation, stemness, invasiveness, and chemoresistance. Therefore, CD44v6 is a promising target for cancer diagnosis and therapy for CRC. In this study, we established anti-CD44 monoclonal antibodies (mAbs) by immunizing mice with CD44v3-10-overexpressed Chinese hamster ovary-K1 (CHO) cells. We then characterized them using enzyme-linked immunosorbent assay, flow cytometry, western blotting, and immunohistochemistry. One of the established clones (C$_{44}$Mab-9; IgG$_1$, kappa) reacted with a peptide of variant 6-encoded region, indicating that C$_{44}$Mab-9 recognizes CD44v6. Furthermore, C$_{44}$Mab-9 reacted with CHO/CD44v3-10 cells or CRC cell lines (COLO201 and COLO205) by flow cytometry. The apparent K_D of C$_{44}$Mab-9 for CHO/CD44v3-10, COLO201, and COLO205 was 8.1×10^{-9} M, 1.7×10^{-8} M, and 2.3×10^{-8} M, respectively. C$_{44}$Mab-9 detected the CD44v3-10 in western blotting, and partially stained the formalin-fixed paraffin-embedded CRC tissues in immunohistochemistry. Collectively, C$_{44}$Mab-9 is useful for detecting CD44v6 in various applications.

Keywords: CD44; CD44v6; monoclonal antibody; colorectal cancer

1. Introduction

Colorectal cancer (CRC) has become the third cancer types for the estimated new cases and deaths in United States, 2022 [1]. The development of CRC is classically explained by Fearon and Vogelstein model; the sequential genetic changes including APC (adenomatous polyposis coli), KRAS, DCC (deleted in colorectal cancer, chromosome 18q), and P53 lead to CRC progression [2]. However, CRC exhibits heterogeneous outcomes and drug responses. Therefore, the large-scale data analysis by an international consortium classified the CRC into four consensus molecular subtypes, including the microsatellite instability immune, the canonical, the metabolic, and the mesenchymal types [3]. In addition, various marker proteins have been investigated for the prediction of prognosis and drug responses of CRC [4,5]. Among them, recent studies suggest that CD44 plays a critical role in tumor progression through its cancer-initiating and metastasis-promoting properties [6].

Preprints (www.preprints.org) | NOT PEER-REVIEWED | Posted: 9 January 2023 doi:10.20944/preprints202301.0153.v1

CD44 is a polymorphic integral membrane protein, which binds to hyaluronic acid, and contributes to cell-matrix adhesion, cell proliferation, migration, and tumor metastasis [7]. When the CD44 is transcribed, its pre-messenger RNA can be received alternative splicing and maturated into mRNAs that encode various CD44 isoforms [8]. The mRNA assembles with ten standard exons and the sixth variant exon encodes CD44v6, which plays critical roles in cell proliferation, migration, survival, and angiogenesis [9,10]. Functionally, CD44v6 can interact with hyaluronic acid (HA) via the standard exons-encoded region [11]. Furthermore, the v6-encoded region functions as a co-receptor of receptor for various cytokines, including epidermal growth factor, hepatocyte growth factor, hepatocyte growth factor, C-X-C motif chemokine 12, and osteopontin [12]. Therefore, the receptor tyrosine kinase or G protein-coupled receptor signaling pathways are potentiated in the presence of CD44v6 [13]. These functions are essential for homeostasis or regeneration in normal tissues. Importantly, CD44v6 overexpression plays a critical role in CRC progression. For instance, CD44v6 confers colorectal carcinoma invasiveness, colonization, and metastasis [14]. Therefore, CD44v6 is a promising target for cancer diagnosis and therapy.

The clinical significance of CD44v6 in CRC deserves consideration. Anti-CD44v6 therapies mainly include the blocking of v6-encoded region by monoclonal antibody (mAb) [12]. First, humanized anti-CD44v6 mAbs (BIWA-4 and BIWA-8) labeled with ^{186}Re exhibited the therapeutic efficacy in head and neck squamous cell carcinoma (SCC) xenograft bearing mice [15]. Furthermore, the humanized anti-CD44v6 mAb, bivatuzumab-mertansine (anti-tubulin agent) conjugate, was evaluated in clinical trials [16]. However, the clinical trials were discontinued due to the severe skin toxicity, including a case of lethal epidermal necrolysis [17]. The efficient accumulation of mertansine was most likely responsible for the high toxicity [17,18]. Therefore, the development of anti-CD44v6 mAbs with more potent and fewer side effects is desired.

We established the novel anti-CD44 mAbs, C$_{44}$Mab-5 (IgG$_1$, kappa) [19] and C$_{44}$Mab-46 (IgG$_1$, kappa) [20] by Cell-Based Immunization and Screening (CBIS) method and immunization of CD44v3-10 ectodomain, respectively. Both C$_{44}$Mab-5 and C$_{44}$Mab-46 recognize the first five standard exons-encoding sequences [21-23]. Therefore, they can recognize both CD44s and CD44v (pan-CD44). Furthermore, C$_{44}$Mab-5 and C$_{44}$Mab-46 exhibited the high reactivity for flow cytometry and immunohistochemical analysis in oral [19] and esophageal [20] SCCs. We also examined the antitumor effects of C$_{44}$Mab-5 in mouse xenograft models [24]. In this study, we developed a novel anti-CD44v6 mAb, C$_{44}$Mab-9 (IgG$_1$, kappa) by CBIS method, and evaluated its applications, including flow cytometry, western blotting, and immunohistochemical analyses.

2. Results

2.1. Establishment of anti-CD44v6 mAb, C$_{44}$Mab-9

We employed the CBIS method to develop anti-CD44 mAbs. In the CBIS method, we prepared a stable transfectant as an immunogen. Then, we performed the high throughput hybridoma screening using flow cytometry (Figure. 1). In this study, mice were immunized with CHO/CD44v3-10 cells. Hybridomas were seeded into 96-well plates, and CHO/CD44v3-10-positive and CHO-K1-negative wells were selected. After limiting dilution, anti-CD44 mAb-producing clones were finally established. Among them, C$_{44}$Mab-9 (IgG$_1$, kappa) was shown to recognize the only CD44p351–370 peptide, which is corresponding to variant 6-encoded sequence (Table 1).

Preprints (www.preprints.org) | NOT PEER-REVIEWED | Posted: 9 January 2023 doi:10.20944/preprints202301.0153.v1

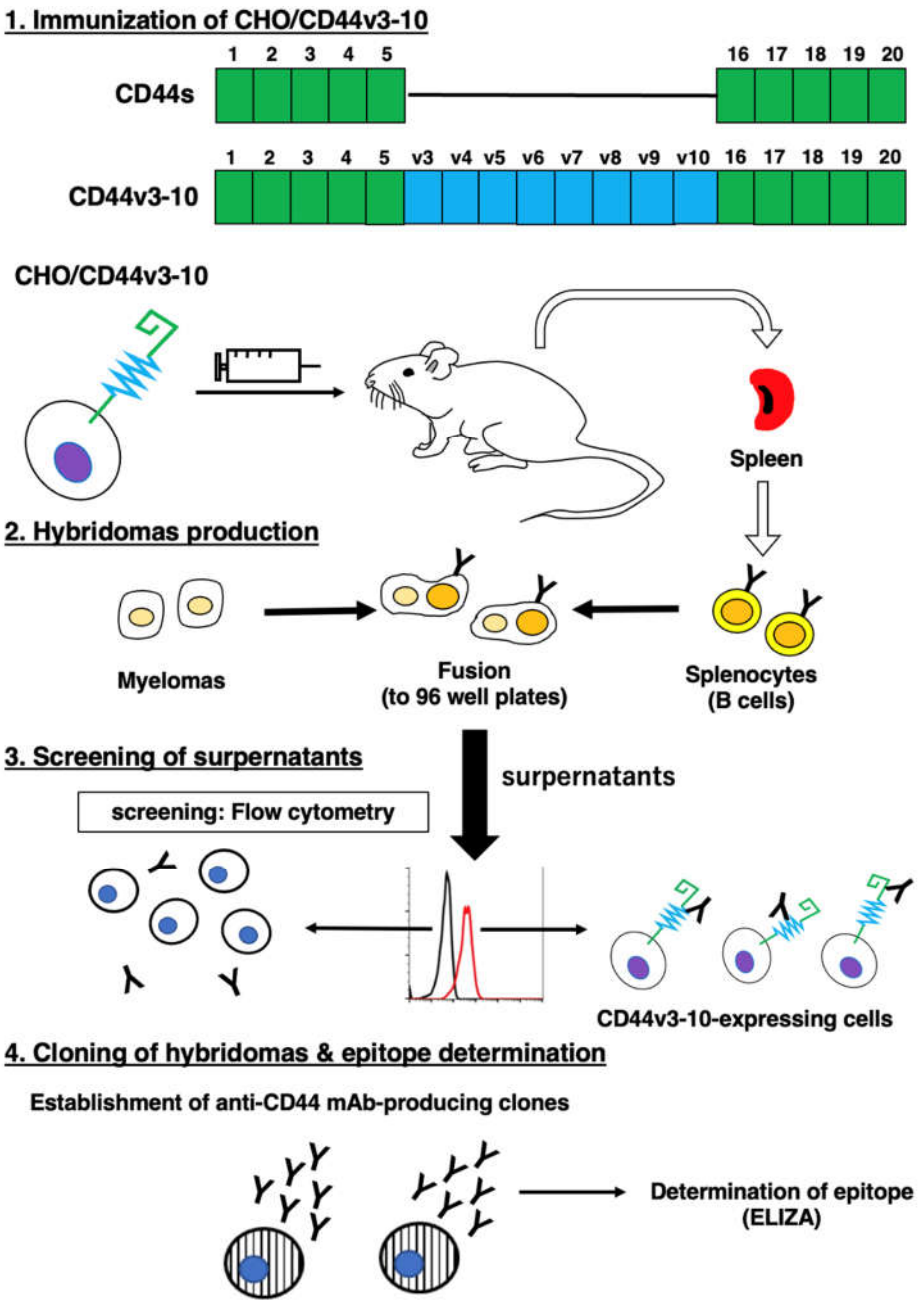

Figure 1. A schematic illustration of ant-human CD44 mAbs production. A BALB/c mouse was intraperitoneally immunized with CHO/CD44v3-10 cells. The screening was then performed by flow cytometry using parental and CHO/CD44v3-10 cells. Finally, the binding epitopes were determined by enzyme-linked immunosorbent assay (ELISA) using peptides which cover the extracellular domain of CD44v3-10.

Preprints (www.preprints.org) | NOT PEER-REVIEWED | Posted: 9 January 2023 doi:10.20944/preprints202301.0153.v1

Table 1. The determination of the binding epitope of C44Mab-9 by ELISA. The CD44 exons are illustrated in Figure 1.

Peptide	Coding exon	Sequence	C44Mab-9
CD44p21–40	2	QIDLNITCRFAGVFHVEKNG	–
CD44p31–50	2	AGVFHVEKNGRYSISRTEAA	–
CD44p41–60	2	RYSISRTEAADLCKAFNSTL	–
CD44p51–70	2	DLCKAFNSTLPTMAQMEKAL	–
CD44p61–80	2/3	PTMAQMEKALSIGFETCRYG	–
CD44p71–90	2/3	SIGFETCRYGFIEGHVVIPR	–
CD44p81–100	3	FIEGHVVIPRIHPNSICAAN	–
CD44p91–110	3	IHPNSICAANNTGVYILTSN	–
CD44p101–120	3	NTGVYILTSNTSQYDTYCFN	–
CD44p111–130	3/4	TSQYDTYCFNASAPPEEDCT	–
CD44p121–140	3/4	ASAPPEEDCTSVTDLPNAFD	–
CD44p131–150	4	SVTDLPNAFDGPITITIVNR	–
CD44p141–160	4	GPITITIVNRDGTRYVQKGE	–
CD44p151–170	4/5	DGTRYVQKGEYRTNPEDIYP	–
CD44p161–180	5	YRTNPEDIYPSNPTDDDVSS	–
CD44p171–190	5	SNPTDDDVSSGSSSERSSTS	–
CD44p181–200	5	GSSSERSSTSGGYIFYTFST	–
CD44p191–210	5	GGYIFYTFSTVHPIPDEDSP	–
CD44p201–220	5	VHPIPDEDSPWITDSTDRIP	–
CD44p211–230	5/v3	WITDSTDRIPATSTSSNTIS	–
CD44p221–240	v3	ATSTSSNTISAGWEPNEENE	–
CD44p231–250	v3	AGWEPNEENEDERDRHLSFS	–
CD44p241–260	v3	DERDRHLSFSGSGIDDDEDF	–
CD44p251–270	v3/v4	GSGIDDDEDFISSTISTTPR	–
CD44p261–280	v4	ISSTISTTPRAFDHTKQNQD	–
CD44p271–290	v4	AFDHTKQNQDWTQWNPSHSN	–
CD44p281–300	v4	WTQWNPSHSNPEVLLQTTTR	–
CD44p291–310	v4	PEVLLQTTTRMTDVDRNGTT	–
CD44p301–320	v4/v5	MTDVDRNGTTAYEGNWNPEA	–
CD44p311–330	v5	AYEGNWNPEAHPPLIHHEHH	–
CD44p321–340	v5	HPPLIHHEHHEEEETPHSTS	–
CD44p331–350	v5/v6	EEEETPHSTSTIQATPSSTT	–
CD44p341–360	v5/v6	TIQATPSSTTEETATQKEQW	–
CD44p351–370	v6	EETATQKEQWFGNRWHEGYR	+
CD44p361–380	v6	FGNRWHEGYRQTPREDSHST	–
CD44p371–390	v6	QTPREDSHSTTGTAAASAHT	–
CD44p381–400	v6/v7	TGTAAASAHTSHPMQGRTTP	–
CD44p391–410	v6/v7	SHPMQGRTTPSPEDSSWTDF	–
CD44p401–420	v7	SPEDSSWTDFFNPISHPMGR	–

Preprints (www.preprints.org) | NOT PEER-REVIEWED | Posted: 9 January 2023 doi:10.20944/preprints202301.0153.v1

CD44p411–430	v7	FNPISHPMGRGHQAGRRMDM	–
CD44p421–440	v7/v8	GHQAGRRMDMDSSHSTTLQP	–
CD44p431–450	v8	DSSHSTTLQPTANPNTGLVE	–
CD44p441–460	v8	TANPNTGLVEDLDRTGPLSM	–
CD44p451–470	v8/v9	DLDRTGPLSMTTQQSNSQSF	–
CD44p461–480	v9	TTQQSNSQSFSTSHEGLEED	–
CD44p471–490	v9	STSHEGLEEDKDHPTTSTLT	–
CD44p481–500	v9/v10	KDHPTTSTLTSSNRNDVTGG	–
CD44p491–510	v10	SSNRNDVTGGRRDPNHSEGS	–
CD44p501–520	v10	RRDPNHSEGSTTLLEGYTSH	–
CD44p511–530	v10	TTLLEGYTSHYPHTKESRTF	–
CD44p521–540	v10	YPHTKESRTFIPVTSAKTGS	–
CD44p531–550	v10	IPVTSAKTGSFGVTAVTVGD	–
CD44p541–560	v10	FGVTAVTVGDSNSNVNRSLS	–
CD44p551–570	v10/16	SNSNVNRSLSGDQDTFHPSG	–
CD44p561–580	v10/16	GDQDTFHPSGGSHTTHGSES	–
CD44p571–590	16	GSHTTHGSESDGHSHGSQEG	–
CD44p581–600	16/17	DGHSHGSQEGGANTTSGPIR	–
CD44p591–606	17	GANTTSGPIRTPQIPEAAAA	–

+, OD655≧0.3; －, OD655<0.1

2.2. Flow Cytometric Analysis of C44Mab-9 to CD44-Expressing Cells

We next confirmed the reactivity of C44Mab-9 against CHO/CD44v3-10 and CHO/CD44s cells by flow cytometry. As shown in Figure 2A, C44Mab-9 recognized CHO/CD44v3-10 cells in a dose-dependent manner, but neither CHO/CD44s (Figure 2B) nor CHO-K1 (Figure 2C) cells. The CHO/CD44s cells were recognized by a pan-CD44 mAb C44Mab-46 [20] (Supplemental Figure S1). Furthermore, C44Mab-9 also recognized endogenous CD44v6 in CRC cell lines as it reacted with both COLO201 (Figure 2D) and COLO205 (Figure 2E) in a dose-dependent manner.

Next, we determined the binding affinity of C44Mab-9 with CHO/CD44v3-10, COLO201, and COLO205 using flow cytometry. The K_D of C44Mab-9 for CHO/CD44v3-10, COLO201, and COLO205 was 8.1×10^{-9} M, 1.7×10^{-8} M, and 2.3×10^{-8} M, respectively, indicating that C44Mab-9 possesses moderate affinity for CD44s-expressing cells (Figure 3).

Preprints (www.preprints.org) | NOT PEER-REVIEWED | Posted: 9 January 2023 doi:10.20944/preprints202301.0153.v1

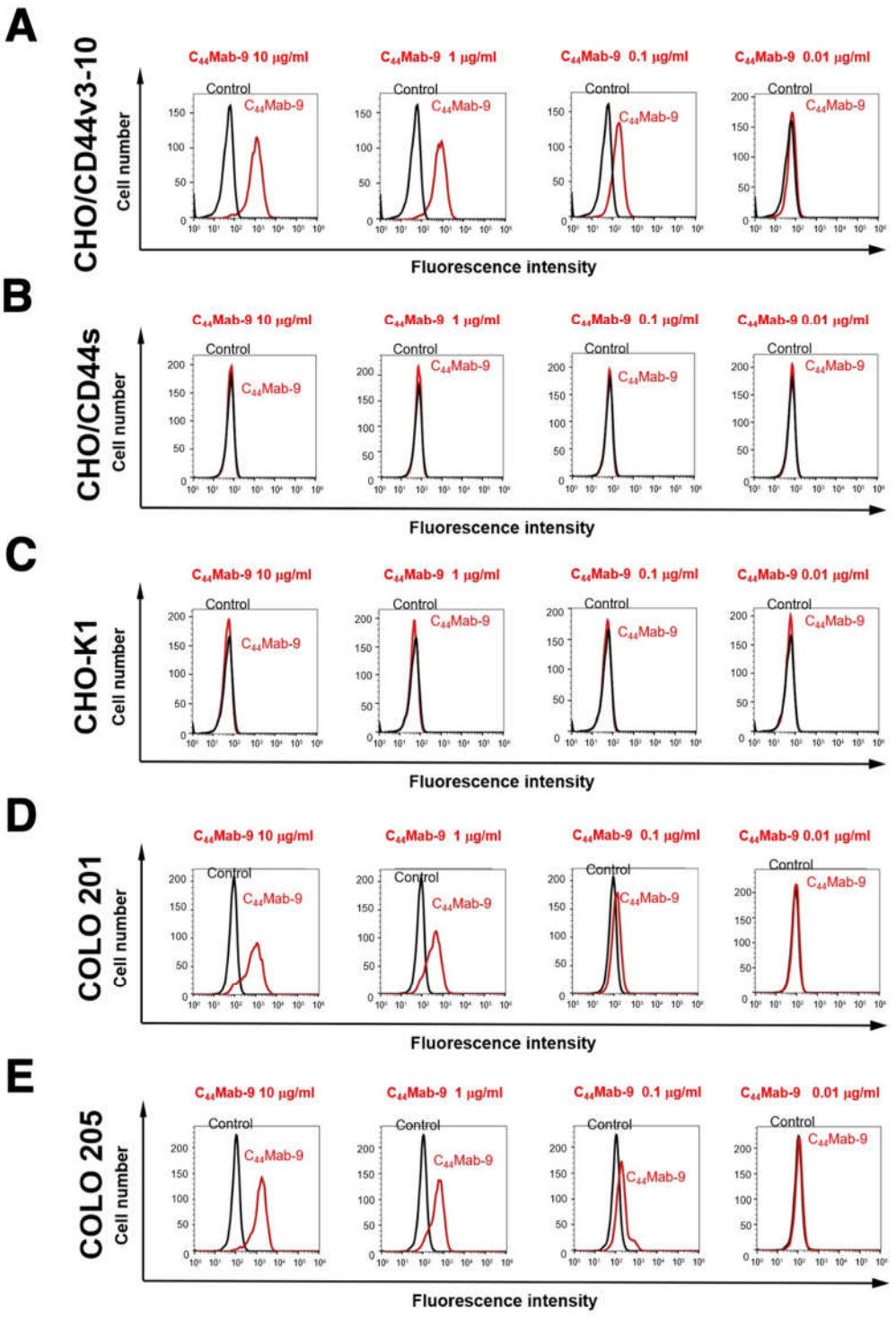

Figure 2. Flow cytometry to CD44-expressing cells using C44Mab-9. CHO/CD44v3-10 (**A**), CHO/CD44s (**B**), CHO-K1 (**C**), COLO201 (**D**), and COLO201 (**E**) were treated with 0.01-10 μg/mL of C44Mab-9, followed by treatment with Alexa Fluor 488-conjugated anti-mouse IgG (Red line). The black line represents the negative control (blocking buffer).

Preprints (www.preprints.org) | NOT PEER-REVIEWED | Posted: 9 January 2023 doi:10.20944/preprints202301.0153.v1

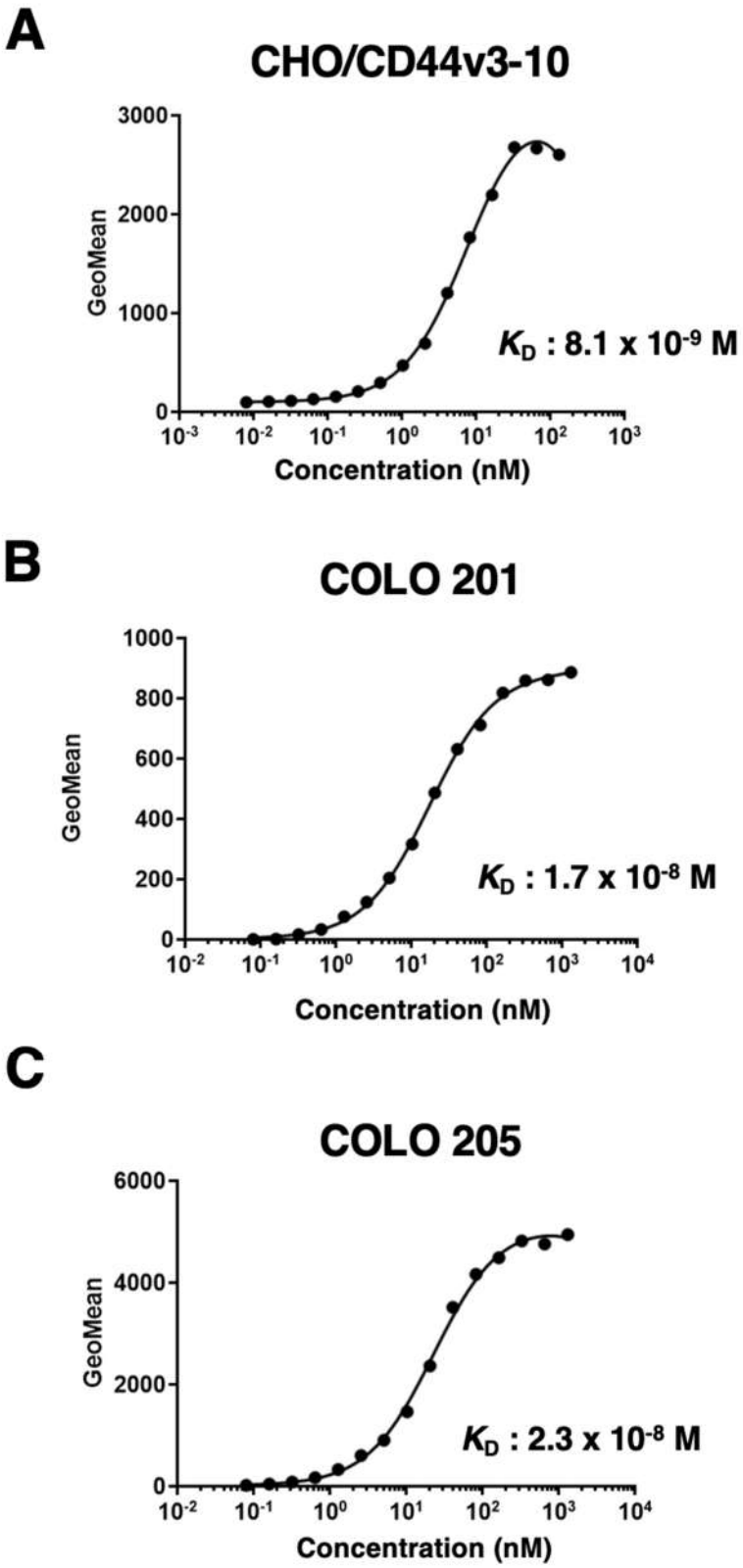

Figure 3. The determination of the binding affinity of C$_{44}$Mab-9 to CD44-expressing cells. CHO/CD44v3-10 (**A**), COLO201 (**B**), and COLO210 (**C**) cells were suspended in 100 μL of serially diluted C$_{44}$Mab-9 (0.08 to 1,300 nM). Then, cells were treated with Alexa Fluor 488-conjugated anti-mouse IgG. Fluorescence data were subsequently collected, followed by the calculation of the apparent dissociation constant (K_D) by GraphPad PRISM 8.

Preprints (www.preprints.org) | NOT PEER-REVIEWED | Posted: 9 January 2023 doi:10.20944/preprints202301.0153.v1

2.3. Western Blot Analysis

We next performed western blotting to assess the sensitivity of C44Mab-9. Total cell lysate of CHO-K1, CHO/CD44s, and CHO/CD44v3-10 were analyzed. As shown in Figure 4, C44Mab-9 detected CD44v3-10 as a more than 180-kDa band. However, C44Mab-9 did not detect any bands from lysates of CHO-K1 and CHO/CD44s cells. An anti-pan-CD44 mAb, C44Mab-46, recognized the lysates from both CHO/CD44s (~75kDa) and CHO/CD44v3-10 (> 180kDa). These results indicated that C44Mab-9 specifically detects exogenous CD44v3-10.

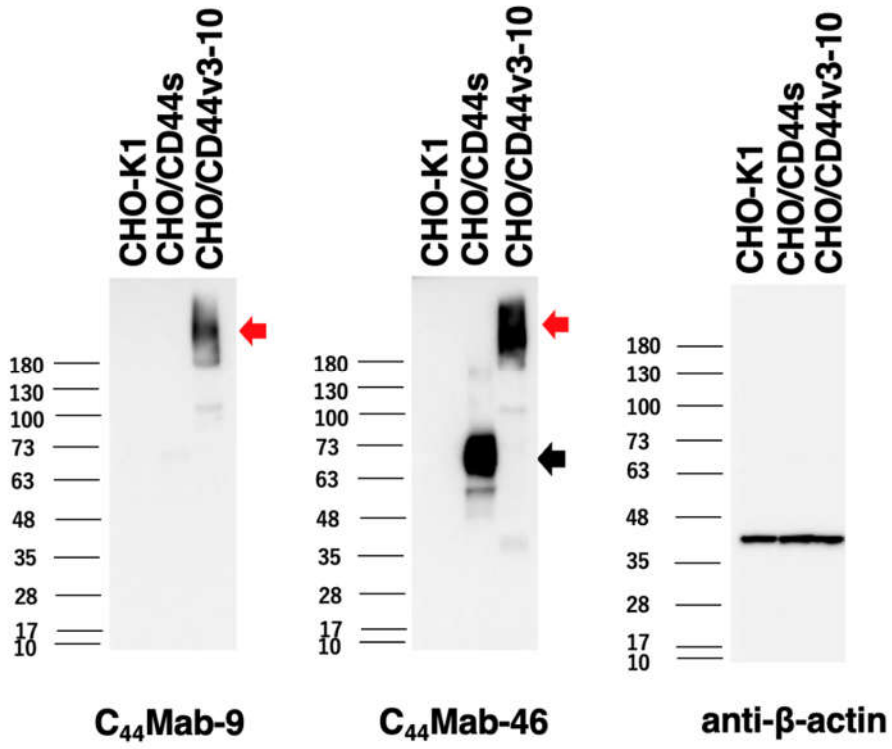

Figure 4. Western blotting by C44Mab-9. The cell lysates of CHO-K1, CHO/CD44s, and CHO/CD44v3-10 (10 μg) were electrophoresed and transferred onto polyvinylidene fluoride (PVDF) membranes. The membranes were incubated with 1 μg/mL of C44Mab-9, 1 μg/mL of C44Mab-46, and 1 μg/mL of anti-β-actin, followed by incubation with peroxidase-conjugated anti-mouse immunoglobulins. The black arrow indicates the CD44s (~75 kDa). The red arrows indicate the CD44v3-10 (>180 kDa).

2.4. Immunohistochemical Analysis Using C44Mab-9 against Tumor Tissues

We next examined whether C44Mab-9 could be used for immunohistochemical analyses using formalin-fixed paraffin-embedded (FFPE) sections. Since previous anti-CD44v6 mAbs could detect CD44v6 in SCC tissues at the high frequency, we first stained an oral SCC tissue. As shown in Figure 5A, C44Mab-9 exhibited a clear membranous staining, and could clearly distinguish tumor cells from stromal tissues. In contrast, C44Mab-46 stained the both (Figure 5B). We next investigated CRC sections. C44Mab-9 showed the membranous staining in CRC cells, but not stromal tissues (Figure 5C). In contrast, C44Mab-46 also stained the both (Figure 5D). These results indicated that C44Mab-9 is useful for immunohistochemical analysis of FFPE tumor sections.

Preprints (www.preprints.org) | NOT PEER-REVIEWED | Posted: 9 January 2023 doi:10.20944/preprints202301.0153.v1

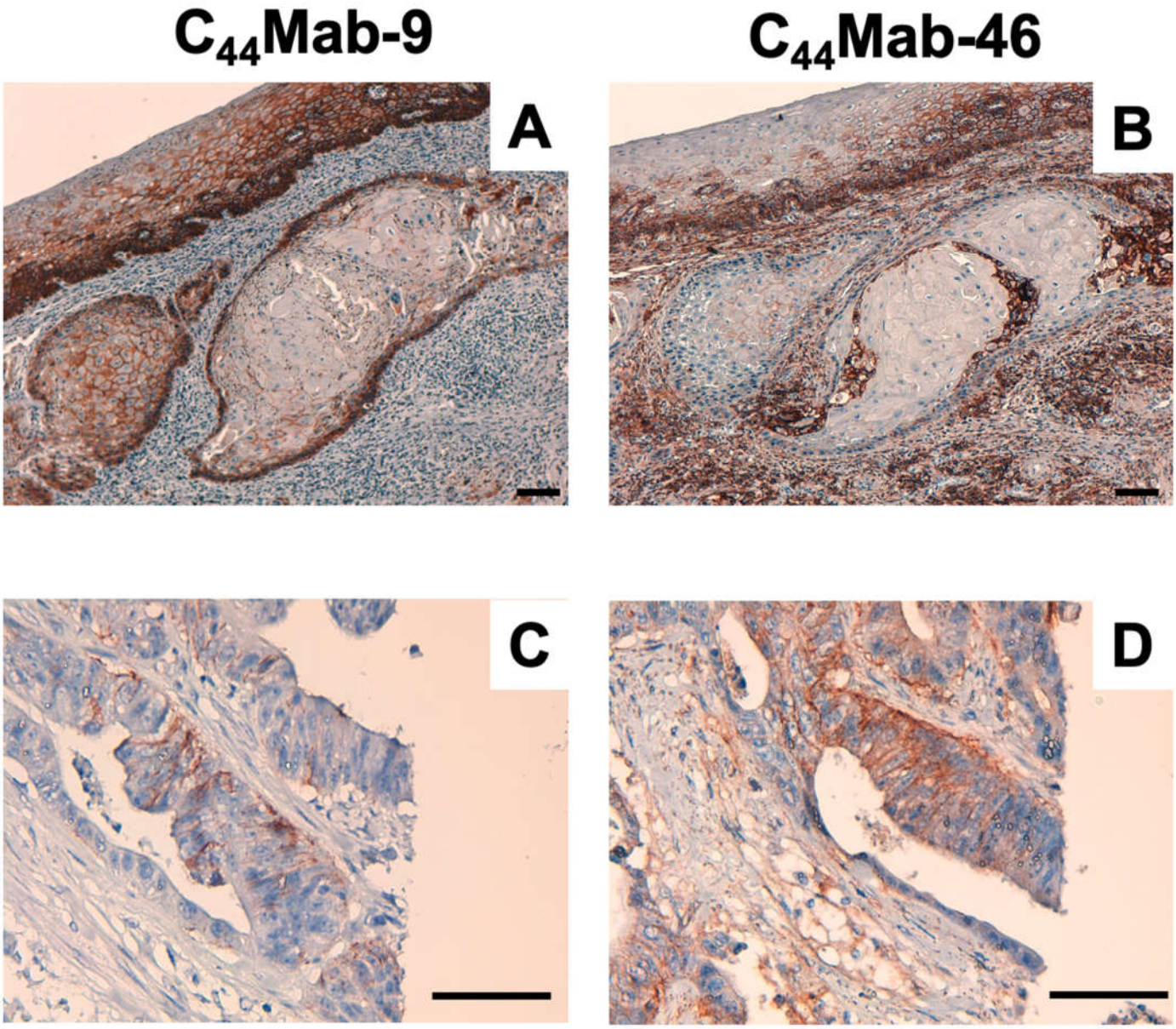

Figure 5. Immunohistochemical analysis using C44Mab-9 and C44Mab-46. (**A**, **B**) Oral SCC sections were incubated with 1 μg/mL of C44Mab-9 (**A**) and C44Mab-46 (**B**). (**C**, **D**) CRC sections were incubated with 1 μg/mL of C44Mab-9 (**C**) and C44Mab-46 (**D**), followed by treatment with the Envision+ kit. Color was developed using DAB, and sections were counterstained with hematoxylin. Scale bar = 100 μm.

3. Discussion

In this study, we developed C44Mab-9 using the CBIS method (Figure 1), and determined its epitope as variant 6 encoded region (Table 1). Then, we showed the usefulness of C44Mab-9 for multiple applications, including flow cytometry (Figure 2 and 3), western blotting (Figure 4), and immunohistochemistry (Figure 5).

Anti-CD44v6 mAbs (clone 2F10 and VFF4, 7, and 18) were previously developed and mainly used for tumor diagnosis and therapy. The 2F10 was established by the immunization of CD44v3-10-Fc protein produced by COS1 cells. The exon specificity of the 2F10 was determined by indirect immunofluorescent staining of COS1 cells transfected with human CD44v cDNAs, including CD44v3-10, CD44v6-10, CD44v7-10, CD44v8-10, and CD44v10 [25]. Therefore, the 2F10 is thought to recognize peptide or glycopeptide structure of CD44v6. However, the detailed binding epitope of 2F10 has not been determined.

Preprints (www.preprints.org) | NOT PEER-REVIEWED | Posted: 9 January 2023 doi:10.20944/preprints202301.0153.v1

The VFF series mAbs were established by the immunization of bacterial expressed CD44v3-10 fused with glutathione *S*-transferase [26,27]. Afterword, VFF4 and VFF 7 were used in immunohistochemical analysis [28], and the VFF18 was humanized as BIWA-4 [15], and developed to bivatuzumab-mertansine drug conjugate for clinical trials [17,18]. The VFF18 bound only to the fusion proteins, containing a variant 6 encoded region. Furthermore, the VFF18 recognized several synthetic peptides, spanning the variant 6 encoded region in ELISA, and the WFGNRWHEGYR peptide was determined as its epitope [26]. As shown in Table 1, C$_{44}$Mab-9 also recognized a synthetic peptide (CD44p351–370), which possesses above sequence. In contrast, a synthetic peptide (CD44p361–380) possesses FGNRWHEGYR sequence, which is not recognized by C$_{44}$Mab-9. Therefore, C$_{44}$Mab-9 and VFF18 recognize CD44v6 with similar variant 6-encoded region. The detailed epitope mapping for C$_{44}$Mab-9 is required in the future.

The clinical significance of CD44v6 expression in patients with CRC using immunohistochemical analysis remain controversial. The elevated expression has been associated with poor prognosis, linked to adverse prognosis [29,30]. However, others have reported that CD44v6 expression is associated with a favorable outcome [31,32]. Various clones of anti-CD44v6 mAbs appeared to influence the outcome of the clinical significance. Among these clinical studies, Saito *et al.* used VFF18 and showed the similar staining patterns of C$_{44}$Mab-9 (Figure 5). They also found that CD44v6 expression was observed in poorly differentiated CRC without E-cadherin expression. Furthermore, the high CD44v6 expression exhibited a significant inverse correlation with E-cadherin expression, and was found to be an independent poor prognostic factor in disease-free survival and overall survival [33]. In the future, we should evaluate the clinical significance of the C$_{44}$Mab-9-positive CRC with E-cadherin expression.

CD44v6-positive CRC cells exhibited cancer-initiating cell property [34]. Cytokines, HGF, C-X-C motif chemokine 12, and osteopontin, secreted from tumor associated fibloblasts, promote the CD44v6 expression in the cancer-initiating cells, which promotes migration and metastasis of CRC cells [14]. Clinically, circulating-tumor cells (CTCs), which express EpCAM, MET, and CD44, identifies a subset with increased metastasis-initiating phenotype [35], suggesting that CD44v6 plays an important role in cancer-initiating cell property cooperating with MET. In addition, CTC culture methods, including two-dimensional (2D) expansion, 3D organoids/spheroids culture, and xenograft formation in mice, have been developed to evaluate the character of CTCs [36]. Therefore, the biological property to affect cell proliferation and invasiveness by C$_{44}$Mab-9 should be investigated because CD44v6 can potentiate the MET signaling by forming the ternary complex with HGF [37]. Therefore, it would be valuable to examine the effect of C$_{44}$Mab-9 on the CTC proliferation *in vitro* and metastasis *in vivo.*

To evaluate the *in vivo* effect, we previously converted the IgG$_1$ subclass of mAbs into a mouse IgG$_{2a}$, and produced a defucosylated version. These defucosylated IgG$_{2a}$ mAbs exhibited potent antibody dependent cellular cytotoxicity *in vitro,* and reduced the tumor growth in mouse xenograft models [38-44]. Therefore, the production of a class switched and defucosylated version of C$_{44}$Mab-9 is required to evaluate the antitumor activity *in vivo*.

4. Materials and Methods

4.1. Cell Lines

Mouse multiple myeloma P3X63Ag8U.1 (P3U1) and CHO-K1 cell lines were obtained from the American Type Culture Collection (ATCC, Manassas, VA, USA). These cells were cultured in RPMI-1640 medium (Nacalai Tesque, Inc., Kyoto, Japan), supplemented with 10% heat-inactivated fetal bovine serum (FBS; Thermo Fisher Scientific, Inc., Waltham, MA, USA), 100 U/mL penicillin, 100 μg/mL streptomycin, and 0.25 μg/mL amphotericin B (Nacalai Tesque, Inc.). Human colorectal cancer cell lines, COLO201 and COLO205 were purchased from ATCC and the Cell Resource Center for Biomedical Research Institute of Development, Aging and Cancer at Tohoku University, respectively.

Preprints (www.preprints.org) | NOT PEER-REVIEWED | Posted: 9 January 2023 doi:10.20944/preprints202301.0153.v1

The COLO201 and COLO205 were cultured in RPMI-1640 medium (Nacalai Tesque, Inc.), supplemented with 10% heat-inactivated FBS, 100 units/ml of penicillin, and 100 μg/ml streptomycin (Nacalai Tesque, Inc.). All the cells were grown in a humidified incubator at 37°C with 5% CO_2.

CD44s cDNA was amplified using HotStar HiFidelity Polymerase Kit (Qiagen Inc., Hilden, Germany) using LN229 cDNA as a template. CD44v3-10 ORF was obtained from the RIKEN BRC through the National Bio-Resource Project of the MEXT, Japan. CD44s and CD44v3-10 cDNAs were subcloned into pCAG-Ble-ssPA16 vector possessing signal sequence and N-terminal PA16 tag (GLEGGVAMPGAEDDVV) [19,45-48], which is detected by NZ-1 [49-64]. CHO/CD44s and CHO/CD44v3-10 were established by transfecting pCAG-Ble/PA16-CD44s and pCAG-Ble/PA16-CD44v3-10 into CHO-K1 cells using a Neon transfection system (Thermo Fisher Scientific, Inc.).

4.2. Hybridoma Production

BALB/c mice (6-weeks old, female) were obtained from CLEA Japan (Tokyo, Japan). The mice were intraperitoneally immunized with CHO/CD44v3-10 (1×10^8 cells) and Imject Alum (Thermo Fisher Scientific Inc.). After three additional immunizations of CHO/CD44v3-10 (1×10^8 cells), a booster injection of CHO/CD44v3-10 was intraperitoneally administered 2 days before harvesting the spleen cells. The splenocytes were fused with P3U1 cells using polyethylene glycol 1500 (PEG1500; Roche Diagnostics, Indianapolis, IN, USA). The hybridomas were cultured in RPMI media supplemented with hypoxanthine, aminopterin, and thymidine (HAT; Thermo Fisher Scientific Inc.) for selection. The culture supernatants were screened using CHO-K1 and CHO/CD44v3-10 by SA3800 Cell Analyzers (Sony Corp. Tokyo, Japan).

4.3. ELISA

Fifty-eight synthesized peptides (Sigma-Aldrich Corp., St. Louis, MO, USA), which cover the CD44v3-10 extracellular domain [21], were immobilized on Nunc Maxisorp 96-well immunoplates (Thermo Fisher Scientific Inc) at a concentration of 1 μg/mL for 30 min at 37 °C. After washing with phosphate-buffered saline (PBS) containing 0.05% (*v*/*v*) Tween 20 (PBST; Nacalai Tesque, Inc.), wells were blocked with 1% (*w*/*v*) bovine serum albumin (BSA)-containing PBST for 30 min at 37°C. C_{44}Mab-9 were added to each well, and then incubated with peroxidase-conjugated anti-mouse immunoglobulins (1:2000 diluted; Agilent Technologies Inc., Santa Clara, CA, USA). Enzymatic reactions were performed using 1 Step Ultra TMB (Thermo Fisher Scientific Inc.). The optical density at 655 nm was mesured using an iMark microplate reader (Bio-Rad Laboratories, Inc., Berkeley, CA, USA).

4.5. Flow Cytometry

CHO-K1 and CHO/CD44v3-10 were isolated using 0.25% trypsin and 1 mM ethylenediamine tetraacetic acid (EDTA; Nacalai Tesque, Inc.) treatment. COLO201 and COLO205 were isolated by brief pipetting. The cells were treated with primary mAbs, or blocking buffer [0.1% bovine serum albumin (BSA; Nacalai Tesque, Inc.) in phosphate-buffered saline (PBS)] (control) for 30 min at 4°C. Subsequently, the cells were incubated in Alexa Fluor 488-conjugated anti-mouse IgG (1:2,000; Cell Signaling Technology, Inc.) for 30 min at 4°C. Fluorescence data were collected using the SA3800 Cell Analyzer and analyzed using SA3800 software ver. 2.05 (Sony Corporation).

4.6. Determination of Dissociation Constant (K_D) by Flow Cytometry

Serially diluted C_{44}Mab-9 was suspended with CHO/EpCAM, COLO201, and COLO205 cells. The cells were further treated with Alexa Fluor 488-conjugated anti-mouse IgG (1:200). Fluorescence data were collected using BD FACSLyric and analyzed using BD FACSuite software version 1.3 (BD Biosciences). To determine the dissociation

constant (K_D), GraphPad Prism 8 (the fitting binding isotherms to built-in one-site binding models; GraphPad Software, Inc., La Jolla, CA, USA) was used.

4.7. Western Blot Analysis

The cell lysates (10 μg of protein) were separated on 5%–20% polyacrylamide gels (FUJIFILM Wako Pure Chemical Corporation, Osaka, Japan) and transferred onto polyvinylidene difluoride (PVDF) membranes (Merck KGaA, Darmstadt, Germany). After blocking (4% skim milk [Nacalai Tesque, Inc.] in PBS with 0.05% Tween 20), the membranes were incubated with 10 μg/mL of C$_{44}$Mab-9 or 1 μg/mL of anti-β-actin (clone AC-15; Sigma-Aldrich Corp.), and then incubated with peroxidase-conjugated anti-mouse immunoglobulins (diluted 1:1,000; Agilent Technologies, Inc.). Finally, the signals were detected with a chemiluminescence reagent, ImmunoStar LD (FUJIFILM Wako Pure Chemical Corporation) using a Sayaca-Imager (DRC Co. Ltd., Tokyo, Japan).

4.8. Immunohistochemical Analysis

The paraffin-embedded oral SCC tissue was obtained from Tokyo Medical and Dental University [65]. Histologic sections of colorectal carcinoma tissue array (Catalog number: CO483a) were purchased from US Biomax Inc. (Rockville, MD, USA). The sections were autoclaved in citrate buffer (pH 6.0; Agilent Technologies Inc.) for 20 min. After blocking with SuperBlock T20 (Thermo Fisher Scientific, Inc.), the sections were incubated with C$_{44}$Mab-9 (1 μg/mL) and C$_{44}$Mab-46 (1 μg/mL) for 1 h at room temperature and then treated with the EnVision+ Kit for mouse (Agilent Technologies Inc.) for 30 min. The color was developed using 3,3′-diaminobenzidine tetrahydrochloride (DAB; Agilent Technologies Inc.) for 2 min. Hematoxylin (FUJIFILM Wako Pure Chemical Corporation) was used for the counterstaining. Leica DMD108 (Leica Microsystems GmbH, Wetzlar, Germany) was used to examine the sections and obtain images.

Supplementary Materials: Figure S1 Conformation of the recognition of CHO/CD44s and CHO/CD44v3-10 by C$_{44}$Mab-46 by flow cytometry.

Author Contributions: R.E., T.T., and T.A. performed the experiments. M.K.K. and Y.K. designed the experiments. R.E. and H.S. analyzed the data. R.E., H.S., and Y.K. wrote the manuscript. All authors have read and agreed to the manuscript.

Funding: This research was supported in part by Japan Agency for Medical Research and Development (AMED) under Grant Numbers: JP22ama121008 (to Y.K.), JP22am0401013 (to Y.K.), JP22bm1004001 (to Y.K.), JP22ck0106730 (to Y.K.), and JP21am0101078 (to Y.K.), and by the Japan Society for the Promotion of Science (JSPS) Grants-in-Aid for Scientific Research (KAKENHI) grant nos. 21K20789 (to T.T.), 22K06995 (to H.S.), 22K15523 (to T.A.), 22K07168 (to M.K.K.), and 22K07224 (to Y.K.).

Institutional Review Board Statement: The animal study protocol was approved by the Animal Care and Use Committee of Tohoku University (Permit number: 2019NiA-001) for studies involving animals.

Acknowledgments: The authors would like to thank Saori Okuno, and Saori Handa (Department of Antibody Drug Development, Tohoku University Graduate School of Medicine) for technical assistance.

Conflicts of Interest: The authors declare no conflicts of interest involving this article.

References

1. Siegel, R.L.; Miller, K.D.; Fuchs, H.E.; Jemal, A. Cancer statistics, 2022. *CA Cancer J Clin* **2022**, *72*, 7-33, doi:10.3322/caac.21708.
2. Fearon, E.R.; Vogelstein, B. A genetic model for colorectal tumorigenesis. *Cell* **1990**, *61*, 759-767, doi:10.1016/0092-8674(90)90186-i.

3. Guinney, J.; Dienstmann, R.; Wang, X.; de Reyniès, A.; Schlicker, A.; Soneson, C.; Marisa, L.; Roepman, P.; Nyamundanda, G.; Angelino, P., et al. The consensus molecular subtypes of colorectal cancer. *Nat Med* **2015**, *21*, 1350-1356, doi:10.1038/nm.3967.
4. Puccini, A.; Seeber, A.; Berger, M.D. Biomarkers in Metastatic Colorectal Cancer: Status Quo and Future Perspective. *Cancers (Basel)* **2022**, *14*, doi:10.3390/cancers14194828.
5. Zöller, M. CD44: can a cancer-initiating cell profit from an abundantly expressed molecule? *Nat Rev Cancer* **2011**, *11*, 254-267, doi:10.1038/nrc3023.
6. Abbasian, M.; Mousavi, E.; Arab-Bafrani, Z.; Sahebkar, A. The most reliable surface marker for the identification of colorectal cancer stem-like cells: A systematic review and meta-analysis. *J Cell Physiol* **2019**, *234*, 8192-8202, doi:10.1002/jcp.27619.
7. Ponta, H.; Sherman, L.; Herrlich, P.A. CD44: from adhesion molecules to signalling regulators. *Nat Rev Mol Cell Biol* **2003**, *4*, 33-45, doi:10.1038/nrm1004.
8. Yan, Y.; Zuo, X.; Wei, D. Concise Review: Emerging Role of CD44 in Cancer Stem Cells: A Promising Biomarker and Therapeutic Target. *Stem Cells Transl Med* **2015**, *4*, 1033-1043, doi:10.5966/sctm.2015-0048.
9. Chen, C.; Zhao, S.; Karnad, A.; Freeman, J.W. The biology and role of CD44 in cancer progression: therapeutic implications. *J Hematol Oncol* **2018**, *11*, 64, doi:10.1186/s13045-018-0605-5.
10. Günthert, U.; Hofmann, M.; Rudy, W.; Reber, S.; Zöller, M.; Haussmann, I.; Matzku, S.; Wenzel, A.; Ponta, H.; Herrlich, P. A new variant of glycoprotein CD44 confers metastatic potential to rat carcinoma cells. *Cell* **1991**, *65*, 13-24, doi:10.1016/0092-8674(91)90403-l.
11. Slevin, M.; Krupinski, J.; Gaffney, J.; Matou, S.; West, D.; Delisser, H.; Savani, R.C.; Kumar, S. Hyaluronan-mediated angiogenesis in vascular disease: uncovering RHAMM and CD44 receptor signaling pathways. *Matrix Biol* **2007**, *26*, 58-68, doi:10.1016/j.matbio.2006.08.261.
12. Ma, L.; Dong, L.; Chang, P. CD44v6 engages in colorectal cancer progression. *Cell Death Dis* **2019**, *10*, 30, doi:10.1038/s41419-018-1265-7.
13. Orian-Rousseau, V.; Morrison, H.; Matzke, A.; Kastilan, T.; Pace, G.; Herrlich, P.; Ponta, H. Hepatocyte growth factor-induced Ras activation requires ERM proteins linked to both CD44v6 and F-actin. *Mol Biol Cell* **2007**, *18*, 76-83, doi:10.1091/mbc.e06-08-0674.
14. Todaro, M.; Gaggianesi, M.; Catalano, V.; Benfante, A.; Iovino, F.; Biffoni, M.; Apuzzo, T.; Sperduti, I.; Volpe, S.; Cocorullo, G., et al. CD44v6 is a marker of constitutive and reprogrammed cancer stem cells driving colon cancer metastasis. *Cell Stem Cell* **2014**, *14*, 342-356, doi:10.1016/j.stem.2014.01.009.
15. Verel, I.; Heider, K.H.; Siegmund, M.; Ostermann, E.; Patzelt, E.; Sproll, M.; Snow, G.B.; Adolf, G.R.; van Dongen, G.A. Tumor targeting properties of monoclonal antibodies with different affinity for target antigen CD44V6 in nude mice bearing head-and-neck cancer xenografts. *Int J Cancer* **2002**, *99*, 396-402, doi:10.1002/ijc.10369.
16. Orian-Rousseau, V.; Ponta, H. Perspectives of CD44 targeting therapies. *Arch Toxicol* **2015**, *89*, 3-14, doi:10.1007/s00204-014-1424-2.
17. Tijink, B.M.; Buter, J.; de Bree, R.; Giaccone, G.; Lang, M.S.; Staab, A.; Leemans, C.R.; van Dongen, G.A. A phase I dose escalation study with anti-CD44v6 bivatuzumab mertansine in patients with incurable squamous cell carcinoma of the head and neck or esophagus. *Clin Cancer Res* **2006**, *12*, 6064-6072, doi:10.1158/1078-0432.Ccr-06-0910.
18. Riechelmann, H.; Sauter, A.; Golze, W.; Hanft, G.; Schroen, C.; Hoermann, K.; Erhardt, T.; Gronau, S. Phase I trial with the CD44v6-targeting immunoconjugate bivatuzumab mertansine in head and neck squamous cell carcinoma. *Oral Oncol* **2008**, *44*, 823-829, doi:10.1016/j.oraloncology.2007.10.009.
19. Yamada, S.; Itai, S.; Nakamura, T.; Yanaka, M.; Kaneko, M.K.; Kato, Y. Detection of high CD44 expression in oral cancers using the novel monoclonal antibody, C(44)Mab-5. *Biochem Biophys Rep* **2018**, *14*, 64-68, doi:10.1016/j.bbrep.2018.03.007.

20. Goto, N.; Suzuki, H.; Tanaka, T.; Asano, T.; Kaneko, M.K.; Kato, Y. Development of a Novel Anti-CD44 Monoclonal Antibody for Multiple Applications against Esophageal Squamous Cell Carcinomas. *Int J Mol Sci* **2022**, *23*, doi:10.3390/ijms23105535.
21. Takei, J.; Asano, T.; Suzuki, H.; Kaneko, M.K.; Kato, Y. Epitope Mapping of the Anti-CD44 Monoclonal Antibody (C44Mab-46) Using Alanine-Scanning Mutagenesis and Surface Plasmon Resonance. *Monoclon Antib Immunodiagn Immunother* **2021**, *40*, 219-226, doi:10.1089/mab.2021.0028.
22. Asano, T.; Kaneko, M.K.; Takei, J.; Tateyama, N.; Kato, Y. Epitope Mapping of the Anti-CD44 Monoclonal Antibody (C44Mab-46) Using the REMAP Method. *Monoclon Antib Immunodiagn Immunother* **2021**, *40*, 156-161, doi:10.1089/mab.2021.0012.
23. Asano, T.; Kaneko, M.K.; Kato, Y. Development of a Novel Epitope Mapping System: RIEDL Insertion for Epitope Mapping Method. *Monoclon Antib Immunodiagn Immunother* **2021**, *40*, 162-167, doi:10.1089/mab.2021.0023.
24. Takei, J.; Kaneko, M.K.; Ohishi, T.; Hosono, H.; Nakamura, T.; Yanaka, M.; Sano, M.; Asano, T.; Sayama, Y.; Kawada, M., et al. A defucosylated antiCD44 monoclonal antibody 5mG2af exerts antitumor effects in mouse xenograft models of oral squamous cell carcinoma. *Oncol Rep* **2020**, *44*, 1949-1960, doi:10.3892/or.2020.7735.
25. Fox, S.B.; Fawcett, J.; Jackson, D.G.; Collins, I.; Gatter, K.C.; Harris, A.L.; Gearing, A.; Simmons, D.L. Normal human tissues, in addition to some tumors, express multiple different CD44 isoforms. *Cancer Res* **1994**, *54*, 4539-4546.
26. Heider, K.H.; Sproll, M.; Susani, S.; Patzelt, E.; Beaumier, P.; Ostermann, E.; Ahorn, H.; Adolf, G.R. Characterization of a high-affinity monoclonal antibody specific for CD44v6 as candidate for immunotherapy of squamous cell carcinomas. *Cancer Immunol Immunother* **1996**, *43*, 245-253, doi:10.1007/s002620050329.
27. Heider, K.H.; Mulder, J.W.; Ostermann, E.; Susani, S.; Patzelt, E.; Pals, S.T.; Adolf, G.R. Splice variants of the cell surface glycoprotein CD44 associated with metastatic tumour cells are expressed in normal tissues of humans and cynomolgus monkeys. *Eur J Cancer* **1995**, *31a*, 2385-2391, doi:10.1016/0959-8049(95)00420-3.
28. Wang, Z.; Tang, Y.; Xie, L.; Huang, A.; Xue, C.; Gu, Z.; Wang, K.; Zong, S. The Prognostic and Clinical Value of CD44 in Colorectal Cancer: A Meta-Analysis. *Front Oncol* **2019**, *9*, 309, doi:10.3389/fonc.2019.00309.
29. Mulder, J.W.; Kruyt, P.M.; Sewnath, M.; Oosting, J.; Seldenrijk, C.A.; Weidema, W.F.; Offerhaus, G.J.; Pals, S.T. Colorectal cancer prognosis and expression of exon-v6-containing CD44 proteins. *Lancet* **1994**, *344*, 1470-1472, doi:10.1016/s0140-6736(94)90290-9.
30. Wielenga, V.J.; Heider, K.H.; Offerhaus, G.J.; Adolf, G.R.; van den Berg, F.M.; Ponta, H.; Herrlich, P.; Pals, S.T. Expression of CD44 variant proteins in human colorectal cancer is related to tumor progression. *Cancer Res* **1993**, *53*, 4754-4756.
31. Zlobec, I.; Günthert, U.; Tornillo, L.; Iezzi, G.; Baumhoer, D.; Terracciano, L.; Lugli, A. Systematic assessment of the prognostic impact of membranous CD44v6 protein expression in colorectal cancer. *Histopathology* **2009**, *55*, 564-575, doi:10.1111/j.1365-2559.2009.03421.x.
32. Nanashima, A.; Yamaguchi, H.; Sawai, T.; Yasutake, T.; Tsuji, T.; Jibiki, M.; Yamaguchi, E.; Nakagoe, T.; Ayabe, H. Expression of adhesion molecules in hepatic metastases of colorectal carcinoma: relationship to primary tumours and prognosis after hepatic resection. *J Gastroenterol Hepatol* **1999**, *14*, 1004-1009, doi:10.1046/j.1440-1746.1999.01991.x.
33. Saito, S.; Okabe, H.; Watanabe, M.; Ishimoto, T.; Iwatsuki, M.; Baba, Y.; Tanaka, Y.; Kurashige, J.; Miyamoto, Y.; Baba, H. CD44v6 expression is related to mesenchymal phenotype and poor prognosis in patients with colorectal cancer. *Oncol Rep* **2013**, *29*, 1570-1578, doi:10.3892/or.2013.2273.
34. Wang, Z.; Zhao, K.; Hackert, T.; Zöller, M. CD44/CD44v6 a Reliable Companion in Cancer-Initiating Cell Maintenance and Tumor Progression. *Front Cell Dev Biol* **2018**, *6*, 97, doi:10.3389/fcell.2018.00097.
35. Baccelli, I.; Schneeweiss, A.; Riethdorf, S.; Stenzinger, A.; Schillert, A.; Vogel, V.; Klein, C.; Saini, M.; Bäuerle, T.; Wallwiener, M., et al. Identification of a population of blood circulating tumor cells from breast cancer patients that initiates metastasis in a xenograft assay. *Nat Biotechnol* **2013**, *31*, 539-544, doi:10.1038/nbt.2576.

36. Rupp, B.; Ball, H.; Wuchu, F.; Nagrath, D.; Nagrath, S. Circulating tumor cells in precision medicine: challenges and opportunities. *Trends Pharmacol Sci* **2022**, *43*, 378-391, doi:10.1016/j.tips.2022.02.005.
37. Orian-Rousseau, V.; Chen, L.; Sleeman, J.P.; Herrlich, P.; Ponta, H. CD44 is required for two consecutive steps in HGF/c-Met signaling. *Genes Dev* **2002**, *16*, 3074-3086, doi:10.1101/gad.242602.
38. Nanamiya, R.; Takei, J.; Ohishi, T.; Asano, T.; Tanaka, T.; Sano, M.; Nakamura, T.; Yanaka, M.; Handa, S.; Tateyama, N., et al. Defucosylated Anti-Epidermal Growth Factor Receptor Monoclonal Antibody (134-mG(2a)-f) Exerts Antitumor Activities in Mouse Xenograft Models of Canine Osteosarcoma. *Monoclon Antib Immunodiagn Immunother* **2022**, *41*, 1-7, doi:10.1089/mab.2021.0036.
39. Kawabata, H.; Suzuki, H.; Ohishi, T.; Kawada, M.; Kaneko, M.K.; Kato, Y. A Defucosylated Mouse Anti-CD10 Monoclonal Antibody (31-mG(2a)-f) Exerts Antitumor Activity in a Mouse Xenograft Model of CD10-Overexpressed Tumors. *Monoclon Antib Immunodiagn Immunother* **2022**, *41*, 59-66, doi:10.1089/mab.2021.0048.
40. Kawabata, H.; Ohishi, T.; Suzuki, H.; Asano, T.; Kawada, M.; Suzuki, H.; Kaneko, M.K.; Kato, Y. A Defucosylated Mouse Anti-CD10 Monoclonal Antibody (31-mG(2a)-f) Exerts Antitumor Activity in a Mouse Xenograft Model of Renal Cell Cancers. *Monoclon Antib Immunodiagn Immunother* **2022**, 10.1089/mab.2021.0049, doi:10.1089/mab.2021.0049.
41. Asano, T.; Tanaka, T.; Suzuki, H.; Li, G.; Ohishi, T.; Kawada, M.; Yoshikawa, T.; Kaneko, M.K.; Kato, Y. A Defucosylated Anti-EpCAM Monoclonal Antibody (EpMab-37-mG(2a)-f) Exerts Antitumor Activity in Xenograft Model. *Antibodies (Basel)* **2022**, *11*, doi:10.3390/antib11040074.
42. Tateyama, N.; Nanamiya, R.; Ohishi, T.; Takei, J.; Nakamura, T.; Yanaka, M.; Hosono, H.; Saito, M.; Asano, T.; Tanaka, T., et al. Defucosylated Anti-Epidermal Growth Factor Receptor Monoclonal Antibody 134-mG(2a)-f Exerts Antitumor Activities in Mouse Xenograft Models of Dog Epidermal Growth Factor Receptor-Overexpressed Cells. *Monoclon Antib Immunodiagn Immunother* **2021**, *40*, 177-183, doi:10.1089/mab.2021.0022.
43. Takei, J.; Ohishi, T.; Kaneko, M.K.; Harada, H.; Kawada, M.; Kato, Y. A defucosylated anti-PD-L1 monoclonal antibody 13-mG(2a)-f exerts antitumor effects in mouse xenograft models of oral squamous cell carcinoma. *Biochem Biophys Rep* **2020**, *24*, 100801, doi:10.1016/j.bbrep.2020.100801.
44. Takei, J.; Kaneko, M.K.; Ohishi, T.; Hosono, H.; Nakamura, T.; Yanaka, M.; Sano, M.; Asano, T.; Sayama, Y.; Kawada, M., et al. A defucosylated anti-CD44 monoclonal antibody 5-mG2a-f exerts antitumor effects in mouse xenograft models of oral squamous cell carcinoma. *Oncol Rep* **2020**, *44*, 1949-1960, doi:10.3892/or.2020.7735.
45. Kato, Y.; Yamada, S.; Furusawa, Y.; Itai, S.; Nakamura, T.; Yanaka, M.; Sano, M.; Harada, H.; Fukui, M.; Kaneko, M.K. PMab-213: A Monoclonal Antibody for Immunohistochemical Analysis Against Pig Podoplanin. *Monoclon Antib Immunodiagn Immunother* **2019**, *38*, 18-24, doi:10.1089/mab.2018.0048.
46. Furusawa, Y.; Yamada, S.; Itai, S.; Sano, M.; Nakamura, T.; Yanaka, M.; Fukui, M.; Harada, H.; Mizuno, T.; Sakai, Y., et al. PMab-210: A Monoclonal Antibody Against Pig Podoplanin. *Monoclon Antib Immunodiagn Immunother* **2019**, *38*, 30-36, doi:10.1089/mab.2018.0038.
47. Furusawa, Y.; Yamada, S.; Itai, S.; Nakamura, T.; Yanaka, M.; Sano, M.; Harada, H.; Fukui, M.; Kaneko, M.K.; Kato, Y. PMab-219: A monoclonal antibody for the immunohistochemical analysis of horse podoplanin. *Biochem Biophys Rep* **2019**, *18*, 100616, doi:10.1016/j.bbrep.2019.01.009.
48. Furusawa, Y.; Yamada, S.; Itai, S.; Nakamura, T.; Takei, J.; Sano, M.; Harada, H.; Fukui, M.; Kaneko, M.K.; Kato, Y. Establishment of a monoclonal antibody PMab-233 for immunohistochemical analysis against Tasmanian devil podoplanin. *Biochem Biophys Rep* **2019**, *18*, 100631, doi:10.1016/j.bbrep.2019.100631.
49. Kato, Y.; Kaneko, M.K.; Kuno, A.; Uchiyama, N.; Amano, K.; Chiba, Y.; Hasegawa, Y.; Hirabayashi, J.; Narimatsu, H.; Mishima, K., et al. Inhibition of tumor cell-induced platelet aggregation using a novel anti-podoplanin antibody reacting with its platelet-aggregation-stimulating domain. *Biochem Biophys Res Commun* **2006**, *349*, 1301-1307, doi:10.1016/j.bbrc.2006.08.171.

50. Chalise, L.; Kato, A.; Ohno, M.; Maeda, S.; Yamamichi, A.; Kuramitsu, S.; Shiina, S.; Takahashi, H.; Ozone, S.; Yamaguchi, J., et al. Efficacy of cancer-specific anti-podoplanin CAR-T cells and oncolytic herpes virus G47Delta combination therapy against glioblastoma. *Mol Ther Oncolytics* **2022**, *26*, 265-274, doi:10.1016/j.omto.2022.07.006.
51. Ishikawa, A.; Waseda, M.; Ishii, T.; Kaneko, M.K.; Kato, Y.; Kaneko, S. Improved anti-solid tumor response by humanized anti-podoplanin chimeric antigen receptor transduced human cytotoxic T cells in an animal model. *Genes Cells* **2022**, *27*, 549-558, doi:10.1111/gtc.12972.
52. Tamura-Sakaguchi, R.; Aruga, R.; Hirose, M.; Ekimoto, T.; Miyake, T.; Hizukuri, Y.; Oi, R.; Kaneko, M.K.; Kato, Y.; Akiyama, Y., et al. Moving toward generalizable NZ-1 labeling for 3D structure determination with optimized epitope-tag insertion. *Acta Crystallogr D Struct Biol* **2021**, *77*, 645-662, doi:10.1107/S2059798321002527.
53. Kaneko, M.K.; Ohishi, T.; Nakamura, T.; Inoue, H.; Takei, J.; Sano, M.; Asano, T.; Sayama, Y.; Hosono, H.; Suzuki, H., et al. Development of Core-Fucose-Deficient Humanized and Chimeric Anti-Human Podoplanin Antibodies. *Monoclon Antib Immunodiagn Immunother* **2020**, *39*, 167-174, doi:10.1089/mab.2020.0019.
54. Fujii, Y.; Matsunaga, Y.; Arimori, T.; Kitago, Y.; Ogasawara, S.; Kaneko, M.K.; Kato, Y.; Takagi, J. Tailored placement of a turn-forming PA tag into the structured domain of a protein to probe its conformational state. *J Cell Sci* **2016**, *129*, 1512-1522, doi:10.1242/jcs.176685.
55. Abe, S.; Kaneko, M.K.; Tsuchihashi, Y.; Izumi, T.; Ogasawara, S.; Okada, N.; Sato, C.; Tobiume, M.; Otsuka, K.; Miyamoto, L., et al. Antitumor effect of novel anti-podoplanin antibody NZ-12 against malignant pleural mesothelioma in an orthotopic xenograft model. *Cancer Sci* **2016**, *107*, 1198-1205, doi:10.1111/cas.12985.
56. Kaneko, M.K.; Abe, S.; Ogasawara, S.; Fujii, Y.; Yamada, S.; Murata, T.; Uchida, H.; Tahara, H.; Nishioka, Y.; Kato, Y. Chimeric Anti-Human Podoplanin Antibody NZ-12 of Lambda Light Chain Exerts Higher Antibody-Dependent Cellular Cytotoxicity and Complement-Dependent Cytotoxicity Compared with NZ-8 of Kappa Light Chain. *Monoclon Antib Immunodiagn Immunother* **2017**, *36*, 25-29, doi:10.1089/mab.2016.0047.
57. Ito, A.; Ohta, M.; Kato, Y.; Inada, S.; Kato, T.; Nakata, S.; Yatabe, Y.; Goto, M.; Kaneda, N.; Kurita, K., et al. A Real-Time Near-Infrared Fluorescence Imaging Method for the Detection of Oral Cancers in Mice Using an Indocyanine Green-Labeled Podoplanin Antibody. *Technol Cancer Res Treat* **2018**, *17*, 1533033818767936, doi:10.1177/1533033818767936.
58. Tamura, R.; Oi, R.; Akashi, S.; Kaneko, M.K.; Kato, Y.; Nogi, T. Application of the NZ-1 Fab as a crystallization chaperone for PA tag-inserted target proteins. *Protein Sci* **2019**, *28*, 823-836, doi:10.1002/pro.3580.
59. Shiina, S.; Ohno, M.; Ohka, F.; Kuramitsu, S.; Yamamichi, A.; Kato, A.; Motomura, K.; Tanahashi, K.; Yamamoto, T.; Watanabe, R., et al. CAR T Cells Targeting Podoplanin Reduce Orthotopic Glioblastomas in Mouse Brains. *Cancer Immunol Res* **2016**, *4*, 259-268, doi:10.1158/2326-6066.CIR-15-0060.
60. Kuwata, T.; Yoneda, K.; Mori, M.; Kanayama, M.; Kuroda, K.; Kaneko, M.K.; Kato, Y.; Tanaka, F. Detection of Circulating Tumor Cells (CTCs) in Malignant Pleural Mesothelioma (MPM) with the "Universal" CTC-Chip and An Anti-Podoplanin Antibody NZ-1.2. *Cells* **2020**, *9*, doi:10.3390/cells9040888.
61. Nishinaga, Y.; Sato, K.; Yasui, H.; Taki, S.; Takahashi, K.; Shimizu, M.; Endo, R.; Koike, C.; Kuramoto, N.; Nakamura, S., et al. Targeted Phototherapy for Malignant Pleural Mesothelioma: Near-Infrared Photoimmunotherapy Targeting Podoplanin. *Cells* **2020**, *9*, doi:10.3390/cells9041019.
62. Fujii, Y.; Kaneko, M.; Neyazaki, M.; Nogi, T.; Kato, Y.; Takagi, J. PA tag: a versatile protein tagging system using a super high affinity antibody against a dodecapeptide derived from human podoplanin. *Protein Expr Purif* **2014**, *95*, 240-247, doi:10.1016/j.pep.2014.01.009.
63. Kato, Y.; Kaneko, M.K.; Kunita, A.; Ito, H.; Kameyama, A.; Ogasawara, S.; Matsuura, N.; Hasegawa, Y.; Suzuki-Inoue, K.; Inoue, O., et al. Molecular analysis of the pathophysiological binding of the platelet aggregation-inducing factor podoplanin to the C-type lectin-like receptor CLEC-2. *Cancer Sci* **2008**, *99*, 54-61, doi:10.1111/j.1349-7006.2007.00634.x.

64. Kato, Y.; Vaidyanathan, G.; Kaneko, M.K.; Mishima, K.; Srivastava, N.; Chandramohan, V.; Pegram, C.; Keir, S.T.; Kuan, C.T.; Bigner, D.D., et al. Evaluation of anti-podoplanin rat monoclonal antibody NZ-1 for targeting malignant gliomas. *Nucl Med Biol* **2010**, *37*, 785-794, doi:10.1016/j.nucmedbio.2010.03.010.

65. Itai, S.; Ohishi, T.; Kaneko, M.K.; Yamada, S.; Abe, S.; Nakamura, T.; Yanaka, M.; Chang, Y.W.; Ohba, S.I.; Nishioka, Y., et al. Anti-podocalyxin antibody exerts antitumor effects via antibody-dependent cellular cytotoxicity in mouse xenograft models of oral squamous cell carcinoma. *Oncotarget* **2018**, *9*, 22480-22497, doi:10.18632/oncotarget.25132.